Monitoring the Microgravity Environment Quality On-Board the International Space Station Using Soft Computing Techniques

Part II: Preliminary System Performance Results

Kenol Jules
Glenn Research Center, Cleveland, Ohio

Paul P. Lin
Cleveland State University, Cleveland, Ohio

Daniel S. Weiss
Harvard University, Cambridge, Massachusetts

August 2002

The NASA STI Program Office . . . in Profile

Since its founding, NASA has been dedicated to the advancement of aeronautics and space science. The NASA Scientific and Technical Information (STI) Program Office plays a key part in helping NASA maintain this important role.

The NASA STI Program Office is operated by Langley Research Center, the Lead Center for NASA's scientific and technical information. The NASA STI Program Office provides access to the NASA STI Database, the largest collection of aeronautical and space science STI in the world. The Program Office is also NASA's institutional mechanism for disseminating the results of its research and development activities. These results are published by NASA in the NASA STI Report Series, which includes the following report types:

- TECHNICAL PUBLICATION. Reports of completed research or a major significant phase of research that present the results of NASA programs and include extensive data or theoretical analysis. Includes compilations of significant scientific and technical data and information deemed to be of continuing reference value. NASA's counterpart of peer-reviewed formal professional papers but has less stringent limitations on manuscript length and extent of graphic presentations.

- TECHNICAL MEMORANDUM. Scientific and technical findings that are preliminary or of specialized interest, e.g., quick release reports, working papers, and bibliographies that contain minimal annotation. Does not contain extensive analysis.

- CONTRACTOR REPORT. Scientific and technical findings by NASA-sponsored contractors and grantees.

- CONFERENCE PUBLICATION. Collected papers from scientific and technical conferences, symposia, seminars, or other meetings sponsored or cosponsored by NASA.

- SPECIAL PUBLICATION. Scientific, technical, or historical information from NASA programs, projects, and missions, often concerned with subjects having substantial public interest.

- TECHNICAL TRANSLATION. English-language translations of foreign scientific and technical material pertinent to NASA's mission.

Specialized services that complement the STI Program Office's diverse offerings include creating custom thesauri, building customized data bases, organizing and publishing research results . . . even providing videos.

For more information about the NASA STI Program Office, see the following:

- Access the NASA STI Program Home Page at *http://www.sti.nasa.gov*

- E-mail your question via the Internet to help@sti.nasa.gov

- Fax your question to the NASA Access Help Desk at 301–621–0134

- Telephone the NASA Access Help Desk at 301–621–0390

- Write to:
  NASA Access Help Desk
  NASA Center for AeroSpace Information
  7121 Standard Drive
  Hanover, MD 21076

Monitoring the Microgravity Environment Quality On-Board the International Space Station Using Soft Computing Techniques

Part II: Preliminary System Performance Results

Kenol Jules
Glenn Research Center, Cleveland, Ohio

Paul P. Lin
Cleveland State University, Cleveland, Ohio

Daniel S. Weiss
Harvard University, Cambridge, Massachusetts

National Aeronautics and
Space Administration

Glenn Research Center

August 2002

Acknowledgments

Monitoring the Microgravity Environment Quality on-board the International Space Station Using Soft Computing Techniques
Part II: Preliminary System Performance Results

Kenol Jules[*]
National Aeronautics and Space Administration
Glenn Research Center
Cleveland, Ohio 44135

Paul P. Lin[†]
Cleveland State University
Cleveland, Ohio 44115

Daniel S. Weiss[‡]
Harvard University
Cambridge, Massachusetts 02138

ABSTRACT

This paper presents the preliminary performance results of the artificial intelligence monitoring system in full operational mode using near real time acceleration data downlinked from the International Space Station. Preliminary microgravity environment characterization analysis result for the International Space Station (Increment-2), using the monitoring system is presented. Also, comparison between the system predicted performance based on ground test data for the U.S. laboratory "Destiny" module and actual on-orbit performance, using measured acceleration data from the U.S. laboratory module of the International Space station is presented. Finally, preliminary on-orbit disturbance magnitude levels are presented for the Experiment of Physics of Colloids in Space, which are compared with on ground test data. The ground test data for the Experiment of Physics of Colloids in Space were acquired from the Microgravity Emission Laboratory, located at the NASA Glenn Research Center, Cleveland, Ohio. The artificial intelligence was developed by the NASA Glenn Principal Investigator Microgravity Services project to help the principal investigator teams identify the primary vibratory disturbance sources that are active, at any moment of time, on-board the International Space Station, which might impact the microgravity environment their experiments are exposed to. From the Principal Investigator Microgravity Services' web site, the principal investigator teams can monitor via a dynamic graphical display, implemented in Java, in near real time, which event (s) is /are on, such as crew activities, pumps, fans, centrifuges, compressor, crew exercise, structural modes, etc., and decide whether or not to run their

experiments, whenever that is an option, based on the acceleration magnitude and frequency sensitivity associated with that experiment.

This monitoring system detects primarily the vibratory disturbance sources. The system has built-in capability to detect both known and unknown vibratory disturbance sources. Several soft computing techniques such as Kohonen's Self-Organizing Feature Map, Learning Vector Quantization, Back-Propagation Neural Networks, and Fuzzy Logic were used to design the system.

INTRODUCTION

The Principal Investigator Microgravity Services (PIMS) project at the NASA Glenn Research Center supports Principal Investigators of the microgravity science community throughout the period of the evaluation of the effects of on-orbit acceleration on their experiments. The Principal Investigator Microgravity Services' primary responsibility is to support NASA sponsored investigators in the area of acceleration data processing and analysis, interpretation and the monitoring of the reduced gravity environment on-board of various carriers.

The residual acceleration environment of an orbiting spacecraft in a low earth orbit is a very complex phenomenon. It is subject to quasi-steady acceleration, higher frequency acceleration, and transient disturbances. Therefore, it is very important that Principal Investigator (PI) teams know what the environment was when their experiments were performed. Without that knowledge, they cannot and will not properly

---

[*] Microgravity Research Scientist
[†] Professor, Mechanical Engineering Department
[‡] Student

account for the effects of on-orbit acceleration disturbances, which are due to the environment of the space-laboratory instead of the phenomenon under study.

Many factors [1], such as experiment operation, life-support systems, equipment operation, crew activities, aerodynamic drag, gravity gradient, rotational effects as well as the vehicle structural resonance frequencies (structural modes) contribute to form the overall reduced gravity environment. Weight-lessness is an ideal state, which cannot be achieved in practice because of the various sources of acceleration present in an orbiting spacecraft. As a result, the environment in which experiments are conducted is *not zero* gravity; therefore, experiments can be affected by the residual acceleration because of their dependency on acceleration magnitude, frequency, orientation and duration. Therefore, experimenters must know what the environment was when their experiments were performed in order to analyze and correctly interpret the result of their experimental data. In a terrestrial laboratory, researchers are expected to know and record certain parameters such as pressure, temperature, humidity level and so on in their laboratory prior to, and possibly throughout their experiment. The same holds true in space, except that acceleration effects emerge as an important consideration.

WHY AN ARTIFICIAL INTELLIGENCE MONITORING SYSTEM

With the International Space Station (ISS) currently operational (starting with flight 6A, which was launched on April 2001), a significant amount of acceleration data is being downlinked and processed daily on ground in an almost continuous basis for both the space station reduced gravity environment characterization (as well as vehicle verification) and scientific experiments. Therefore, to help principal investigator teams monitor the reduced gravity acceleration level on-board the ISS (and ease the PIMS' data analyst daily task) in order to understand and avoid undesirable impact on their experiment, when possible, the NASA Glenn Principal Investigator Microgravity Services (PIMS) project developed an Artificial Intelligence (AI) monitoring system, which detects in near real time any change in the reduced gravity environment susceptible to affect PIs' experiments.

SYSTEM OBJECTIVE

The main objective of this monitoring system is to help the principal investigator teams, in near real time, identify the primary vibratory disturbance sources that are active at any instant of time on-board the ISS, which might impact the reduced gravity environment their experiments are exposed to. The soft computing techniques, which are used, consist of an adaptive pattern classification, which is a hybrid of Kohonen's Self-Organizing Feature Map (SOFM), Learning Vector Quantization (LVQ), Back Propagation Neural Networks (BPNN), and fuzzy logic [2]. This monitoring system allows any principal investigator team, at any location and at any time, to see the current acceleration level, for the vibratory regimes, on-board the Space Station via the World Wide Web. From the Principal Investigator Microgravity Services' web site, the principal investigator teams can see in

near real time which event (s) is/are active, such as crew activity, pumps, fans, centrifuges, compressor, crew exercise, structural modes, reboost, extra-vehicular activity, etc., and decide whether or not to run their experiments based on the g-level associated with a specific event. A dynamic graphical display, implemented in Java, via the World Wide Web shows the status of all the vibratory disturbance sources with their degree of confidence as well as their impact on the reduced gravity environment. Part I of this paper, which was presented at the 51st International Astronautical Federation (IAF) Congress [3], in Brazil (2001), covered the system design. Part II focuses essentially on the performance and analysis capability of the system in full operational mode using live data downlinked from the Station. Preliminary reduced gravity environment characterization of the ISS-Increment-2 analysis result, using the AI monitoring system, is presented. Also, comparison between the system predicted performance and actual performance, using measured data on-board the station, is presented. Finally, preliminary on-orbit disturbance magnitude levels are presented for the Experiment of Physics of Colloids in Space (EXPPCS), which are compared with on ground test data. This monitoring system detects primarily vibratory disturbance sources. The system identifies both known and unknown vibratory disturbance sources to accommodate the incremental build-up nature of the Station.

In summary, the Microgravity Environment Monitoring System (MEMS) performs the following tasks: 1) detect the current vibratory events on-board the ISS in near real time; 2) classify each known event and assess their relative impact on the environment; 3) identify unknown events, which require characterization. The system acts as the ISS microgravity environment analyzer for the PIs, thus freeing them from the burden of being a reduced gravity environment analyst so that they can concentrate on running / analyzing their experiments. It is important to note that the MEMS' main focus is the vibratory regime.

ACCELEROMETERS

To provide support for the science experiments, which require acceleration data measurement on the ISS, the NASA Physical Science Division sponsors two microgravity accelerometers; Space Acceleration Measurement System (SAMS) and Microgravity Acceleration Measurement System (MAMS). SAMS measures vibratory acceleration data in the range of 0.01 to 400 Hz for payloads requiring such measurement [4]. MAMS consists of two sensors. MAMS-OARE Sensor Subsystem (OSS), a low frequency range sensor (DC to 1 Hz), is used to characterize the quasi-steady environment for payloads and the vehicle (ISS) and MAMS-High Resolution Accelerometer Package (HiRAP) is used to characterize the ISS vibratory environment up to 100 Hz [5]. Both accelerometers were flown to the ISS on the Space Transportation System (STS-100), which was launched April 19, 2001, from the Kennedy Space Center (KSC). The preliminary results reported in this paper were obtained using both MAMS-HiRAP and SAMS accelerometer systems. The preliminary results presented covered the time period of

May 11th to June 8th, 2001, [6] for which acceleration data were measured from the ISS using both systems.

OVERALL SYSTEM DESCRIPTION

Due to the complexity associated with designing this system, three artificial neural networks techniques [7–10] were combined: SOFM, LVQ and BPNN (Fig. 1). In addition to these three techniques, fuzzy logic [11] was used to deal with the system fuzziness. For a complete description on how these techniques were used in the system design and integration see reference [3].

The system is designed to operate mainly in two modes: 1.) Microgravity mode, and 2.) Non-microgravity mode. An in-depth description of the particular of these two modes relating to the ISS operation, can be found in references [12,13]. For reference 13, see Table 4. In brief, the microgravity mode, which is specified only for the ISS configuration at assembly complete, should last for 180 days per year in continuous time intervals of at least 30 days. During that time intervals certain operations or events, which are detrimental to the reduced gravity environment are not allowed. Those events are allowed only during the non-microgravity mode. The AI system captures both operation modes. The system is set up to perform both on-line and off-line processing. In the on-line processing mode, the system detects all incoming events it is trained for, while in the off-line mode, the system identifies all incoming unknown patterns, which the on-line mode have not yet trained for [3]. The system's default operating mode is the dual mode (the system performs both tasks simultaneously).

DYNAMIC GRAPHICAL DISPLAY

This section provides a brief overview of the dynamic graphical display module, which allows PIs to assess the reduced gravity environment level, in near real time. The module has two main components: a *Graph Applet* which displays the data and can be accessed by the users via the World Wide Web, and a *Data Server* which supplies data to the Graph Applet. The module is implemented in Java due to its portability and platform-independence.

The Graph Applet

The Graph Applet is responsible for dynamically displaying the current ISS environment data. The Graph Applet is an extension of the Applet class, a native Java class that provides the functionality to embed the program within an hypertext mark-up language (HTML) page and access it via the World Wide Web.

The Graph Applet has three main components: a drop-down menu that allows the user to select the sensor to be monitored, a panel used to display messages on the screen, and a set of bar graphs, each of which displays data for a single ISS event. Along with each bar graph are four buttons: *sensor_id*, *x-axis*, *y-axis* and *z-axis* (Figure 3). Clicking the *sensor_id* button for an event calls up a diagram showing where the

accelerometer reporting on the event is located; clicking on an *axis* buttons shows a data log for that axis.

The Data Server

Due to data transmission restrictions placed on Applets, they are only allowed to make network connections to the machine from which they are being served. This means that it is impossible for Graph Applet clients to connect directly to the Microgravity Environment Monitoring System (MEMS) data server, which provides the actual ISS vibratory disturbance data, instead they are connected to a Data Server program which runs on their host machine and acts as a pipeline to the MEMS data server. Therefore, they are two data server: an internal one and an external one.

Configuration Data

In order to determine which events need to be displayed for each sensor, the Graph Applets consult a set of configuration files that store the frequency range for each sensor and event. An event is displayed for a given sensor if its frequency range overlaps the sensor's frequency range by at least 75 percent. These configuration files can be changed on the fly. At any time the system administrator can use the External Server to issue a reload command to the Graph Applet clients that instructs them to use whatever new values have been stored in the configuration data files.

Network Protocols

Communications between the MEMS data server and Internal Server, as well as between the Internal Server and External Server, use the transmission control protocol /internet protocol (TCP/IP). This protocol provides guaranteed packet delivery along these channels. However, TCP/IP is not well suited for communications between the External Server and Graph Applet clients because it requires a separate threaded socket for each connection, which would unduly tax system resources for large numbers of clients. Instead, these communications rely on the user datagram protocol (UDP) and use liveness countdowns and regularly generated packets from the clients to ensure that data is successfully propagated throughout the system.

PSD DATA DESCRIPTION

The Power Spectral Density [14,15] (PSD) is a frequency domain function, which is often used to indicate the dominant frequency components present in the data. PSD analysis is performed on time series data to identify the relative magnitudes of sinusoidal signals that compose the series. The basis of this computation is the Fourier transform [16], which gives an estimate of the distribution of power with respect to frequency in the acceleration signal. PIMS analysts use the discrete Fourier transform of a time series such that Parseval's relation is satisfied: the root means square (RMS) of a time signal is equal to the square root of the integral of the PSD across the frequency band represented by the original signal.

ISS MEMS uses the PSD data to detect the characteristic frequency of each event using a peak detector algorithm in order to identify all incoming learned patterns. All unknown patterns are handed over to the off-line mode of MEMS for further analysis (Fig. 2).

POWER SPECTRAL DENSITY VERSUS TIME (SPECTROGRAM)

Color spectrograms provide a road map of how acceleration signals vary with respect to both time and frequency. To produce a spectrogram, PSDs are computed for successive intervals of time. The PSDs are oriented vertically on a page such that frequency increases from bottom to top. PSDs from successive time slices are aligned horizontally across the page such that time increases from left to right. Each time-frequency bin is imaged as a color corresponding to the base 10 logarithm of the PSD magnitude at that time and frequency. Spectrograms are particularly useful for identifying structure and boundaries in time and frequency over relatively long periods of time [14,15]. All of the data (MAMS-HiRAP and SAMS) presented in this paper were obtained by inspecting visually many color spectrogram plots over a 10-day period to determine which strips of the spectrogram plots need to be analyzed for specific frequency range.

DATA REDUCTION AND ANALYSIS

In order to perform the analysis, which generates the results presented below, many spectrograms were generated to qualitatively assess when a certain event took place during the 10-day period for which acceleration data were collected aboard the ISS. Once the spectrograms were generated, visual inspections were made to select which specific time segments from the spectrograms PSDs should be generated for, from which the adaptive pattern recognition and classification (APRC) can extract the needed information to perform the identification and classification analysis. For a sampling rate of 1,000 samples per seconds, it took the software generating the PDSs 8 seconds using 8,193 points for a frequency spectrum of 0 to 100 Hz for each PSD. To reduce spectral variance, spectral averaging of 10 consecutive frames was used. Once the PSDs are generated, APRC begins with a peak detector algorithm, which detects all the major peaks of that PSD set. Each PSD set is made of x, y and z-axes. For the 10-day period, a total of 3600 patterns for each axis were detected (a total of 10,800 for all three axes). A pattern, for example for the x-axis, contents the frequency detected along with the acceleration level for that event. The patterns for all three axes were identified and classified as unknown.

The patterns were further classified as narrow or broad bands. Narrow band is defined as any detected frequency, whose deviation is no more than $\pm \Delta f$ (one frequency resolution—$\Delta f = \pm .122$ Hz for this work) from its nominal frequency; broadband otherwise. For the broadband case, the median frequency as well as the lowest and the highest values are reported. For each acceleration level associated with a detected frequency, in both narrow and broad bands, the lowest as well as the highest acceleration values are reported.

Once all the 10,800 patterns were classified, all the detected peaks verified with PSDs and spectrograms, patterns were sorted out and tables generated for all three axes as reported below.

Microgravity vibration environment tests were conducted on the U.S. laboratory module (Destiny), at KSC during December 1999 and in February 2000. For this test the U.S. Lab module was configured in the stage 6A on-orbit configuration with all the eleven (11) system racks. All equipment racks were outfitted with their appropriate on-orbit equipment. The U.S. Lab system racks house 129 potential sources of disturbance. The largest four potential disturbers are: the pump package assembly (PPA) and the temperature/humidity control (THC) cabin air fan located in the rack # 6 on the port side; the PPA located in rack # 6 on the starboard; and the avionics air assembly (AAA) fan located in rack # 6 on the floor or deck. All system equipment such as pumps and fans, except the carbon dioxide removal assembly (CDRA), were operational. The international standard payload racks (ISPR) were not installed in the U.S. Lab during this test (thirteen locations are reserved for ISPR racks). For more information regarding the U.S. Lab KSC microgravity test, the readers should refer to [17–20].

The test data were obtained from the Boeing Company. The data were in the form of constant narrowband PSD and one-third octave band amplitude-frequency spectra. The sampling rate was fixed during data acquisition at 1024 samples per second. Both background and baseline noise measurements were taken. Background data usually refers to measurements that are due to the ambient building source. No U.S. Lab equipment was running during these measurements. Baseline refers to data taken before a lab measurement. Baseline noise was measured with both space station processing facility (SSPF) and the U.S. Lab external support equipment operating, but with all interior U.S. Lab equipment shut down. The U.S. Lab external support equipment includes the following: 2 chiller pumps on cooling servicer, large vacuum pump, power supplies, computers and 2 ground support equipment coolant circulation pumps (during some runs). For the data presented below regarding the U.S. Lab ground data, the baseline noise measurements were removed.

DISCUSSION AND CONCLUSION

This paper presents some preliminary results, which assess the ISS microgravity environment, in order to share with the microgravity scientific community what is currently being observed in terms of disturbances aboard the ISS. It must be pointed out that the ISS microgravity environment characterization is at an early stage, therefore, not too much is known with certainty. To give the microgravity scientific community some ideas of the daunting task of characterizing such a complex platform, many sets of data are used, such as MAMS-HiRAP, SAMS, actual on-orbit payload (experiment) performance, which are compared with on ground test data in order to assess the on ground versus on-orbit performance deviation. More specifically, actual comparisons are made using the U.S. Laboratory "Destiny" ground test result, which was performed at Kennedy Space Center (KSC) in December

1999 and February 2000, with actual on-orbit measured data. Also, EXPPCS on-orbit performance (how loud or quiet it is) is compared with ground test, which was performed in the Microgravity Emission Lab (MEL) on May 4–5, 2000, at NASA Glenn Research Center. The results presented here are *VERY* preliminary since we are in the early stage of receiving, processing, analyzing, digesting and comparing the data. There are more questions at this stage than answers. With that in mind, let's discuss the significance of the results presented below in this paper.

Table 1 shows both acceleration levels and frequencies for different activities recorded by MAMS-HiRAP aboard the ISS over a 10-day period. The table shows activities, which are observed only on the X, Y and Z-axes of the MAMS-HiRAP, respectively. Then, activities observed on two axes, and finally, on all three axes. This is very important for experiments, which have directional and/or frequency sensitivities. It is very important to note that these data are presented in the MAMS-HiRAP on-orbit coordinate systems [21]. The table provides information such as the nature of the disturbance detected (narrow or broadband). In the case of the broadband, the frequency range (low and high end) is provided; also, the median acceleration level is provided along with the lowest and the highest level of acceleration detected for that specific activity over the 10-day period. Finally, a column, which lists some comments, provides some speculations on what that specific activity might be. We have reasons to believe that most of them are correct, but since this is a preliminary look at the data, we will call them "speculation" at this point, until more in-depth analysis is performed.

Table 2 presents the same type of data, but for a different accelerometer, SAMS, for head 121f06, which was located in EXPRESS rack 2, mounted on the EXPPCS [22,23] test section. MAMS-HiRAP was located in EXPRESS rack 1, which is a non-isolated (meaning a non-Active Rack Isolation System (ARIS)) rack, while the SAMS sensor head used to collect the data presented in this table was located in an ARIS rack (rack 2). An ARIS rack is designed to attenuate the disturbance effects onboard the ISS within a specified frequency band (0.01 to 1 Hz or 2 Hz dependent on rack optimization configuration); they may be vehicle structural modes or other disturbances cause by experiments not located in an ARIS rack. Therefore, Table 2 is an eye-bird view of what an ARIS[‡] rack detects compared to a non-ARIS rack (Table 1). The detail explanation of the difference in the environment seen by these two racks is beyond the scope of this paper. Again, it must be pointed out that the data presented in Table 2 is in SAMS' head 121f06 on-orbit coordinate systems [22], which is not the same with MAMS-HiRAP. MAMS-HiRAP on-orbit +X-axis corresponds to SAMS' 121f06 on-orbit -Z-axis, HiRAP -Y-axis corresponds to SAMS' 121f06 -Y-axis and HiRAP -Z-axis corresponds to SAMS' 121f06 -X-axis [21].

Table 3 presents the result of the U.S. Lab "Destiny" ground test performed at KSC. The result is the reduced data. Baseline noise measurements have been removed from the on ground measured data. Table 3 is provided as a comparison between what was measured on-ground and what is actually being detected on-orbit (Tables 1 and 2). Table 3 shows the signature (frequency) of the different equipments such as fans, pumps, and blower, located throughout the U.S. Laboratory. Notice that Table 3 is equipment and axis specific. The U.S.-ISS analysis coordinate system was used for the sensors orientation during the ground test of the U.S. module. The axes comparison between Table 3 (ground test) and Tables 1 and 2 (MAMS-HiRAP and SAMS 121f06) are as follow: $+X_A$ (ISS analysis X-axis) corresponds to $+X_H$ (HiRAP) and $-Z_{f06}$ (SAMS); $+Y_A$ corresponds to $-Y_H$ and $-Y_{f06}$; $+Z_A$ corresponds to $-Z_H$ and $-X_{f06}$.

Table 4 shows the actual acceleration level (on ground) when all the equipments aboard the U.S. laboratory were switched on except for one: the Carbon Dioxide Removal Assembly (CDRA) fan. The addition of the CDRA fan does not contribute much to the environment. Table 4 shows frequencies with associated acceleration levels for the microgravity disturbers in the U.S. Lab for X, Y and Z-axes, respectively.

Figures 4–6 show the on-orbit versus on-ground disturbance levels of the EXPPCS payload (experiment) measured by MAMS-HiRAP and SAMS 121f06 (for both on-orbit data and on ground). The flight unit, with SAMS 121f06 head mounted exactly as the on-orbit configuration, was ground tested before flying to ISS. As was mentioned before, the ground data was taken from the microgravity emission lab (MEL) at NASA Glenn. The EXPPCS experiment contains eight different colloid samples. Each sample consists of a fluid and solid particle mixture. The mix/melt operation was performed many times on-orbit with the longest period of operation of 5 hours in a given day. Most mix/melt operations is on the order of 5 minutes with the initial sedimentation mixes to eliminate sedimentation taking up to 30 minutes each. The operation is performed to eliminate sedimentation and aggregation of particles and to disperse the solid particles throughout the fluid. This operation consists of quickly oscillating the sample cell via a DC motor and belt system [24].

From Figures 4–6, the plots labeled Mix/Melt and sedimentation are the on ground test data measured from the MEL for these two operation modes, while the SAMS 121f06 and MAMS-HiRAP data were measured at the same time (on-orbit) at two different locations on the ISS. The on-orbit data is mainly Mix/Melt operations (how much is sedimentation is not known since no information in that regard was available during that segment of on-orbit operation). The data measured by MAMS-HiRAP was up to 100 Hz (that is HiRAP cut off frequency). SAMS 121f06 head was mounted directly on the EXPPCS test section (the same configuration with the ground test in the MEL), while HiRAP was located approximately 42.5 inches away from the SAMS 121f06 head. Note that a much higher magnitude level was measured on ground than

---

[‡] Timeline information regarding which mode ARIS was in during the time period considered here was not available at the moment this paper was written.

on-orbit. Another significance of Figures 4–6 is that they show the on-orbit magnitude attenuation (or on-orbit transfer functions) since SAMS 121f06 and HiRAP measurements were taken from two different racks (the two sensors were located 42.5 inches). Note that Figure 5 shows only SAMS and MAMS-HiRAP on-orbit data. This is due to the fact that no Y-axis data was available for the MEL ground test.

It is our hope that soon we will be able to identify most of the signatures listed in the tables presented in this paper. We hope that this paper will help shedding some lights on the complexity involved in characterizing the ISS and also the result presented will start a meaningful discussion within the microgravity scientific community as to how best to use the data to start removing some of the uncertainties associated with the prediction/simulation tools for the ISS.

REFERENCES

1. Hamacher, H., Fluid Sciences and Materials Science in Space, Spring-Verlag, 1987.

2. Lin, P.P., and Jules, K., "An intelligent System for Monitoring the Microgravity Environment Quality on-board the International Space Station," IEEE Instrumentation and Measurement Technology Conference 2001, Vol. 3., pp. 2117–2122, Budapest.

3. Jules, K., and Lin, P.P., "Monitoring the Microgravity Environment Quality On-board the International Space Station Using Soft Computing Techniques—Part I: System Design," IAF-00-J.5.06, October 2000, Rio de Janeiro, Brazil.

4. Space Acceleration Measurement System II, RTS SE Electronic Test Report, SE 121-Q02, SAMS-II 657-RPT1, NASA, December 2000.

5. "Microgravity Acceleration Measurement System for the International Space Station," Canopus Systems Inc., CSI 0101 MAMS TR008, Contract No: NAS3–26556, May 2001.

6. PIMS on-console log book, May–June, NASA Glenn Research Center, Cleveland, Ohio, May–June 2001.

7. Haykin, S., Neural Networks: A Comprehensive Foundation, Prentice Hall, Inc., 1994.

8. Kohonen, T., "Improved Versions of Learning Vector Quantization," International Joint Conference on Neural Networks, V.1, pp. 545–550, San Diego, 1990.

9. Kohonen, T., "Learning Vector Quantization for Pattern Recognition," Technical Report TKK-F-A601, Helsinki University of technology, Finland, 1986.

10. Freeman, J.A., and Skapura, D.M., "Neural Network: Algorithms, Applications, and Programming Techniques," Addison-Wesley Publishing Company, Inc., 1991.

11. Jang, J.S., and Gulley, N., Application of Fuzzy Logic in Control Design, Technical Brief, Mathworks Inc., 1996.

12. Microgravity Analysis Integration Team, "Microgravity Control Plan (Revision B)", Report No: SSP-50036B, The Boeing Company, Houston, TX, NASA—Contract No. NAS15–1000 (Drive-16), February 1999.

13. International Space Station User's Guide Release 2.0, NASA.

14. Rogers, J.B. Melissa et al. "Analysis Techniques for Residual Acceleration Data", NASA–TM 103507, July 1990.

15. Rogers, J.B. Melissa., Hrovat, Kenneth et al. "Accelerometer Data Analysis and Presentation Techniques," NASA–TM 113173, September 1997

16. Moskowitz, E. Milton., Hrovat, Kenneth et al. "Summary Report of Mission Acceleration Measurements for MSL-1," NASA–TM 206979, May 1998.

17. O. Crenwelge., "U.S. Lab Microgravity Test: Low Frequency Mode Resolution", Boeing, SSP-MG00-034, April 25, 2000.

18. E. O'keefe., V. Shekher., "ISS Lab Microgravity Vibration Environment Measurements and SEA Model Comparisons." AIAA–2001–6406.

19. O. Crenwelge., E. O'Keefe., "U.S. Lab Microgravity Test: Quick-Look Test and Data Report," Boeing, SSP-MG00-013, February 28, 2000.

20. V. Shekher., "U.S. Lab Microgravity Disturbance Prediction Correlation with KSC Test Measurements, Revision 1," V Memo #: 2-8V6C-VS-009/00, Rev 1, June 2, 2000.

21. K. Jules., K. Hrovat., E. Kelly., "International Space Station Increment-2 Quick Look Report," NASA/TM–2002-211200, January 2002.

22. K. Jules et al. "International Space Station Increment-2 Microgravity Environment Summary Report," NASA/TM—2002-211335, January 2002.

23. http://www.grc.nasa.gov/WWW/PAO/PAIS/fs12grc.htm or http://www.spaceref.com/iss/payloads/exppcs.html

24. M. Houston., A. McNelis., "Microgravity Emission Lab
    Reprot for the Physics of Colloids in Space (PCS)
    Experiment and Avionics Packages," NASA-MEL-TR
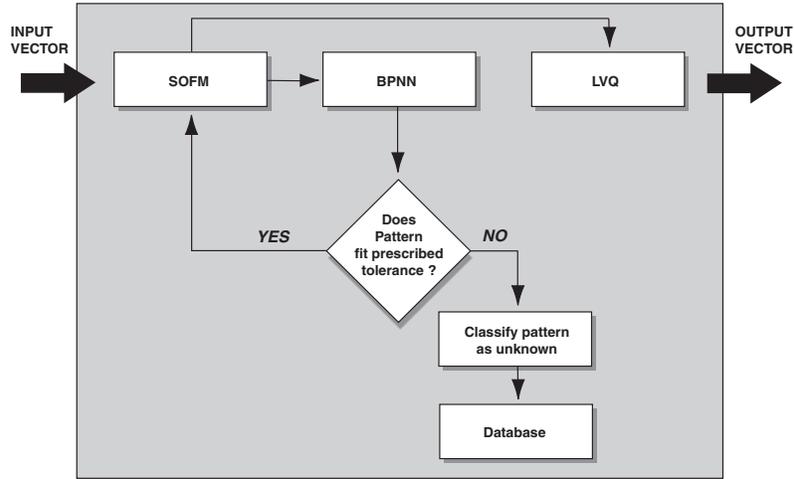   00-04, January 30, 2001.

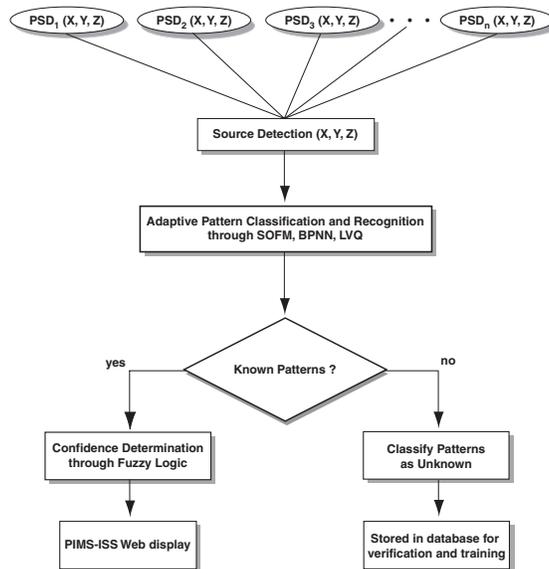Figure 1: Adaptive Pattern Recognition and Classification (APRC)

Figure 2: MEMS-ISS overall environment Characterization Flowchart
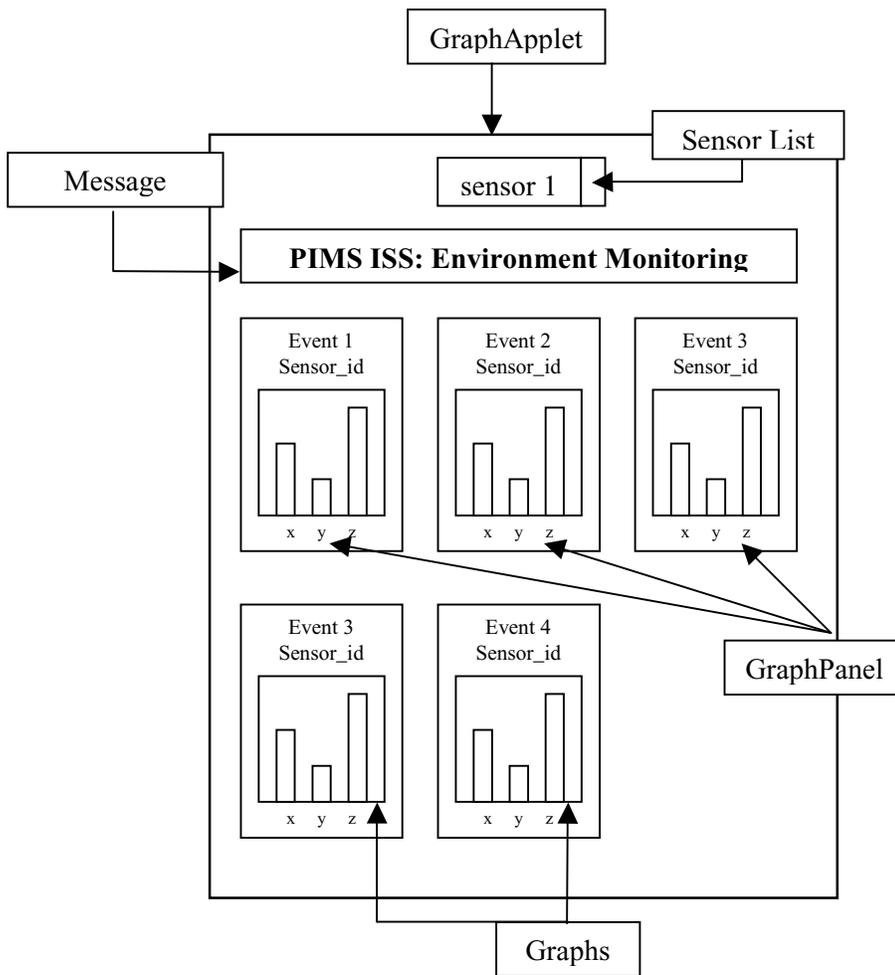
Figure 3: Layout of the MEMS-ISS Web Dynamic Graphical Display

Table 1: Frequencies Identification of the MEMS System for ISS Increment-2 over a 10-day period

Nominal Frequency (Hz)	Low end (Hz)	High end (Hz)	Band type	Median Level (µg)	Low end (µg)	High end (µg)	Excitation level (µg)	Comment
MAMS-HiRAP: X-axis only								
1.8311			Narrow	27	8.4121	88.892		Structural
3.7842			Narrow	65	6.9859	121.09	188.93	Structural
4.6387			Narrow	50	21.582	111.43		Structural
11.597			Narrow	20	7.1607	48.046		
13.672			Narrow	30	5.0939	69.260		
14.404			Narrow	51	17.729	84.30		
15.137			Narrow	59	16.879	84.536		
15.991			Narrow	28	15.855	72.29	162.14	
16.602			Narrow	30	5.9014	62.211		
18.677	18.818	19.531	Broadband	21	8.8645	37.908		
MAMS-HiRAP: Z-axis only								
5.9814	5.8594	6.2256	Broadband	16	10.398	17.775	185.04	Structural
7.5684			Narrow	8	5.2704	12.047	171.64	Structural
MAMS-HiRAP: X and Z-axes								
0.97656 (x)			Narrow	14.8	4.8229	43.306		Structural
0.97656 (z)			Narrow	33	8.0831	65.824		Structural
39.185 (x)			Narrow	9.0	5.7623	15.071		
39.185 (z)	38.82	41.75	Broadband	5.0	3.2659	10.555		
MAMS-HiRAP: Y and Z-axes								
9.5215 (y)	9.1553	9.887	Broadband	17	3.2905	54.391		
9.5215 (z)	9.2773	9.644	Broadband	30	4.6486	87.878		
15.625 (y)	15.259	15.99	Broadband	19	7.3364	46.698		
15.625 (z)	15.015	15.99	Broadband	36	8.9874	74.023		
83.984 (y)			Narrow	30	7.5534	34.195		EXPPCS
83.984 (z)			Narrow	25	21.413	34.03		EXPPCS

Table 1: Concluded.

Nominal Frequency (Hz)	Low end (Hz)	High end (Hz)	Band type	Median Level (µg)	Low end (µg)	High end (µg)	Excitation level (µg)	Comment
MAMS-HiRAP: X, Y and Z-axes								
.48828 (x)			Narrow	8.50	4.2772	22.628		Structural
.48828 (y)			Narrow	43.0	5.6869	108.69	180.59	Structural
.48828 (z)			Narrow	40.0	6.9941	74.655		Structural
1.3428 (x)			Narrow	16.0	5.1388	46.174		Structural
1.3428 (y)			Narrow	10.0	5.7588	20.517		Structural
1.3428 (z)			Narrow	30.0	3.3875	68.281		Structural
2.5635 (x)			Narrow	40.0	8.6313	109.56	195.83	Structural
2.5635 (y)			Narrow	17.5	3.9494	34.825		Structural
2.5635 (z)			Narrow	80.4	55.104	105.66		Structural
6.4697 (x)	5.127	7.446	Broadband	124.0	13.372	284.35		Structural
6.4697 (y)	5.9814	6.854	Broadband	21.0	8.3173	56.712		Structural
6.4697 (z)	6.3477	6.958	Broadband	16.0	5.1989	29.329		Structural
7.8125 (x)			Narrow	199.0	14.995	401.54		
7.8125 (y)			Narrow	45.0	8.9089	86.141		
7.8125 (z)			Narrow	40.0	5.736	91.883		
10.376 (x)			Narrow	29.0	5.6605	56.275		
10.376 (y)			Narrow	60.0	18.339	98.514		
10.376 (z)			Narrow	54.0	4.316	117.39		
11.353 (x)			Narrow	10.5	4.1704	47.326		
11.353 (y)			Narrow	16.9	12.896	20.916		
11.353 (z)			Narrow	58.0	8.5245	72.184		
11.963 (x)			Narrow	27.0	20.233	50.008		EXPPCS
11.963 (y)			Narrow	12.6	3.8082	24.39		EXPPCS
11.963 (z)			Narrow	28.0	6.7884	49.333		EXPPCS
13.184 (x)	12.695	13.428	Broadband	12.0	4.7207	29.494		
13.184 (y)	12.695	13.92	Broadband	33.0	14.753	67.404		
13.184 (z)	12.695	13.92	Broadband	50.0	18.984	85.7		
20.508 (x)	19.653	21.12	Broadband	13.0	4.1738	31.446		
20.508 (y)	19.775	21.36	Broadband	28.0	12.098	53.542		
20.508 (z)	19.653	20.63	Broadband	28.0	8.8437	60.844		
23.438 (x)			Narrow	15.0	5.4083	27.038		SKV-1
23.438 (y)			Narrow	32.0	15.789	64.198		SKV-1
23.438 (z)			Narrow	24.0	12.60	54.73		SKV-1
26.367 (x)	25.879	27.47	Broadband	6.0	4.1576	13.496		
26.367 (y)	25.391	27.34	Broadband	42.0	6.2566	100.07		
26.367 (z)	25.391	27.222	Broadband	23.0	6.4870	45.569		
49.438 (x)			Narrow	10.0	8.1438	15.896		
49.438 (y)			Narrow	43.0	35.041	51.334		
49.438 (z)			Narrow	16.0	12.400	18.216		
57.617 (x)			Narrow	250.0	161.3	393.98		ADVASC
57.617 (y)			Narrow	519.0	323.77	711.12		ADVASC
57.617 (z)			Narrow	222.0	136.83	305.99		ADVASC
61.401 (x)	60.913	61.401	Broadband	11.80	7.3783	20.117		
61.401 (y)	60.425	62.988	Broadband	29.0	15.709	59.83		
61.401 (z)	60.547	62.378	Broadband	21.0	9.3832	29.381		
67.749 (x)			Narrow	98.0	68.329	129.25		
67.749 (y)			Narrow	132.0	114.42	181.34		
67.749 (z)			Narrow	51.0	39.852	74.975		
69.458 (x)	68.359	69.824	Broadband	195.0	108.24	334.13		
69.458 (y)	68.97	69.702	Broadband	270.0	166.62	498.39		
69.458 (z)	68.848	69.946	Broadband	66.0	31.245	125.52		
75.684 (x)	74.585	78.125	Broadband	353.0	154.72	854.39		ADVASC
75.684 (y)	74.707	77.026	Broadband	200.0	92.32	587.84		A DVASC
75.684 (z)	74.829	77.271	Broadband	329.0	70.549	508.64		ADVASC
87.769 (x)	87.036	88.013	Broadband	270.0	129.87	445.75		ADVASC
87.769 (y)	86.914	88.013	Broadband	60.0	41.699	76.801		ADVASC
87.769 (z)	86.914	88.013	Broadband	67.0	49.281	93.112		ADVASC
96.069 (x)			Narrow	150.0	18.838	290.15	625.59	EXPPCS
96.069 (y)			Narrow	30.4	7.9412	67.442		EXPPCS
96.069 (z)			Narrow	35.0	8.522	89.861	148.02	EXPPCS

Table 2: Frequencies Identification of the MEMS System for ISS Increment-2 for SAMS-121f06

Nominal Frequency (Hz)	Low end (Hz)	High end (Hz)	Band type	Median Level (µg)	Low end (µg)	High end (µg)	Excitation level (µg)	Comment
SAMS-121f06: X-axis only								
1.2207			Narrow	14.276	12.848	15.704		Structural
6.958			Narrow	22.60	20.34	24.86		
97.00	97.29	97.92	Broadband	37.051	23.591	50.51		EXPPCS ?
SAMS-121f06: Y-axis only								
0.48828			Narrow	49.498	18.837	80.16		Structural
4.3945	4.1504	4.6387	Broadband	33.181	27.644	38.718		
7.0801			Narrow	19.602	17.642	21.562		
7.9345			Narrow	18.936	14.313	23.559		
9.3994			Narrow	14.527	13.074	15.979		
10.62			Narrow	10.062	9.0558	11.068		
19.836			Narrow	2.431	2.1828	2.6791		
24.78			Narrow	5.7657	4.7662	6.7652		
95.337			Narrow	26.318	10.242	42.395		EXPPCS ?
SAMS-121f06: Z-axis only								
0.12207			Narrow	2.3896	2.1506	2.6283		Structural
0.36621			Narrow	7.1522	6.4369	7.8674		Structural
0.97656			Narrow	22.305	20.074	24.535		Structural
1.709			Narrow	3.4192	3.0773	3.7611		Structural
6.3476			Narrow	31.809	15.986	47.633		
7.8125			Narrow	18.431	6.4848	30.377		
18.500			Narrow	2.1915	1.9723	2.4106		
SAMS-121f06: X and Y-axes								
1.0986 (x)			Narrow	63.033	56.728	69.336		Structural
1.0986 (y)			Narrow	19.778	17.800	21.756		Structural
5.8594 (x)			Narrow	72.285	47.012	97.574		
5.8594 (y)			Narrow	55.202	37.463	72.947		
17.578 (x)	17.092	17.94	Broadband	1.1125	0.9293	1.2958		
17.578 (y)			Narrow	1.4052	1.0265	1.5457		
51.391 (x)			Narrow	2.0688	1.8619	2.2757		
51.391 (y)			Narrow	11.284	10.156	12.412		
SAMS-121f06: X and Z-axes								
0.8545 (x)			Narrow	20.251	18.226	22.276		Structural
0.8545 (z)			Narrow	13.400	6.2693	20.531		Structural
1.3428 (x)			Narrow	21.374	19.237	23.511		Structural
1.3428 (z)			Narrow	4.3815	3.9433	4.8196		Structural
2.6855 (x)			Narrow	60.906	54.815	66.996		
2.6855 (z)			Narrow	26.684	22.619	30.749		
9.5215 (x)			Narrow	8.5605	7.7044	9.4165		
9.5215 (z)			Narrow	28.756	25.880	31.632		
SAMS-121f06: Y and Z-axes								
76.294 (y)			Narrow	11.047	10.857	11.238		
76.294 (z)			Narrow	10.736	9.7225	11.751		
93.000 (y)	92.895	93.75	Broadband	58.252	55.994	60.511		
93.000 (z)	92.895	93.23	Broadband	79.823	71.841	87.805		

Table 2: Concluded.

			SAMS-121f06: X, Y and Z-axes					
Nominal Frequency (Hz)	Low end (Hz)	High end (Hz)	Band type	Median Level (µg)	Low end (µg)	High end (µg)	Excitation level (µg)	Comment
2.3193 (x)			Narrow	86.328	77.695	94.961		Structural
2.3193 (y)	2.3193	2.4414	Broadband	40.206	23.171	57.241		Structural
2.3193 (z)			Narrow	166.13	149.52	182.74		Structural
11.597 (x)			Narrow	9.517	7.0646	11.969		
11.597 (y)	11.475	11.719	Broadband	35.328	20.133	50.523		
11.597 (z)	11.475	11.963	Broadband	27.507	17.242	37.772		
23.437 (x)			Narrow	0.9508	0.8210	1.0805		SKV-1
23.437 (y)			Narrow	4.2956	3.7491	4.8422		SKV-1
23.437 (z)			Narrow	2.3649	1.1736	3.5562		SKV-1
26.489 (x)			Narrow	1.3839	1.2455	1.5229		
26.489 (y)			Narrow	5.2389	4.7150	5.7628		
26.489 (z)	24.780	26.850	Broadband	1.7697	1.5927	1.9467		
46.265 (x)			Narrow	32.336	28.729	35.944		
46.265 (y)	45.776	46.446	Broadband	11.272	9.7991	12.744		
46.265 (z)	46.02	46.300	Broadband	9.3771	7.3253	11.429		
54.321 (x)			Narrow	3.0549	2.0538	4.056		
54.321 (y)			Narrow	11.678	10.510	12.846		
54.321 (z)			Narrow	6.2332	5.8437	6.6228		
56.03 (x)			Narrow	4.0949	3.6854	4.5044		
56.03 (y)			Narrow	14.236	12.236	15.659		
56.03 (z)			Narrow	26.485	24.580	28.391		
57.739 (x)			Narrow	6.6837	6.0153	7.3521		
57.739 (y)			Narrow	33.219	26.313	40.125		
57.739 (z)			Narrow	29.649	26.867	32.612		
59.204 (x)			Narrow	3.7446	3.3701	4.1191		
59.204 (y)			Narrow	22.784	22.177	23.391		
59.204 (z)			Narrow	27.085	26.479	27.691		
61.401 (x)			Narrow	5.3333	2.8005	7.8662		
61.401 (y)			Narrow	20.036	18.097	21.975		
61.401(z)			Narrow	13.404	10.870	15.938		
69.582 (x)	69.214	69.985	Broadband	4.4686	4.0217	4.9155		
69.582 (y)			Narrow	9.8242	8.8418	10.807		
69.582 (z)	69.421	70.434	Broadband	7.3622	6.2759	8.4486		
81.665 (x)			Narrow	26.589	24.831	28.348		
81.665 (y)			Narrow	25.335	22.105	28.565		
81.665 (z)			Narrow	42.363	32.576	52.151		
85.937 (x)			Narrow	6.0024	5.4022	6.6026		
85.937 (y)			Narrow	11.105	9.9945	12.215		
85.937 (z)			Narrow	32.258	26.359	38.157		
99.487 (x)			Narrow	37.051	23.591	50.51		
99.487 (y)	99.400	99.853	Broadband	38.58	37.121	40.039		
99.487 (z)	99.400	99.731	Broadband	80.248	49.047	111.45		

Table 3: U.S. Laboratory "Destiny" Microgravity Ground Test Single Disturbers Responses

U.S. Lab: Pump Package Assembly (PPA)

X-axis		Y-axis		Z-axis	
Frequency (Hz)	Acceleration (µg)	Frequency (Hz)	Acceleration (µg)	Frequency (Hz)	Acceleration (µg)
41	103	41	121	64	66
71	218	45.75	125	71	66
140.25	1268	64.75	242	86.5	85
280.5	2851	82.5	223	92.5	91
		91.25	264	129	36
		106	287	140.25	686
		128.75	64	173	12
		140.25	541	280.5	3104
		280.5	9497		

U.S. Lab: Common Cabin Air Assembly (CCAA) Fan

X-axis		Y-axis		Z-axis	
Frequency (Hz)	Acceleration (µg)	Frequency (Hz)	Acceleration (µg)	Frequency (Hz)	Acceleration (µg)
40.75	80	40.75	30	41	39
82.5	40	82.5	64	82.75	24
103	1280	86	141	86.0	49
190.75	147	95.25	543	95.25	168
206.25	1306	103	1280	103	1235
278.5	177	190.75	110	190.75	108
		206	1306	206.25	1444
		260.75	174	260.5	341
		278.5	317	278.5	194

U.S. Lab: Avionics Air Assembly (AAA) Fan

X-axis		Y-axis		Z-axis	
Freq uency (Hz)	Acceleration (µg)	Frequency (Hz)	Acceleration (µg)	Frequency (Hz)	Acceleration (µg)
29.5	73	29.5	40	29.5	21
50.75	104	50.75	108	50.75	718
61.25	59	61.25	78	61.25	153
82.75	70	86.5	48	82.75	145
86.5	42	101.5	40	86.5	85
101.5	17	152.25	13	101.5	128
120	22.9	173	25	152.25	13
		193.75	50	165.75	24
		225.25	28	173	12

U.S. Lab: Carbon Dioxide Removal Assembly (CDRA) Blower

X-axis		Y-axis		Z-axis	
Frequency (Hz)	Acceleration (µg)	Frequency (Hz)	Acceleration (µg)	Frequency (Hz)	Acceleration (µg)
50.75	192	50.75	404	50.75	137
101.5	49	101.5	218	101.5	17

U.S. Lab: Trace Contaminant Control System (TCCS) Blower

X-axis		Y-axis		Z-axis	
Frequency (Hz)	Acceleration (µg)	Frequency (Hz)	Acceleration (µg)	Frequency (Hz)	Acceleration (µg)
40.75	173.61	46.75	201	50.25	139
82.5	474	64	700	64	213
127	393	86.75	555	86.75	240
142	920	104.75	574	104.75	205
284	1787	127	123	127.25	103
		142	465	142	427
		284	4957	284	2009

U.S. Lab: Intermodule Ventilation System (IMV) Fan

X-axis		Y-axis		Z-axis	
Frequency (Hz)	Acceleration (µg)	Frequency (Hz)	Acceleration (µg)	Frequency (Hz)	Acceleration (µg)
20.75	17	29	15	29.5	55
29.5	11	58.25	211	59.75	14
41.25	14	69.25	35	71	6
59.75	20	112.5	21	120	5
84.5	5	138.75	23	141.5	12
112.5	28	160.25	31	238	10
119.75	13	225.25	13	277.5	19
141.5	11	276.5	24		
160.25	13				
174.75	9				
225.25	9				
239.75	12				
247.5	34				
277.5	10				

Table 4: U.S. Laboratory "Destiny" Microgravity Ground Test, all sources active, except CDRA

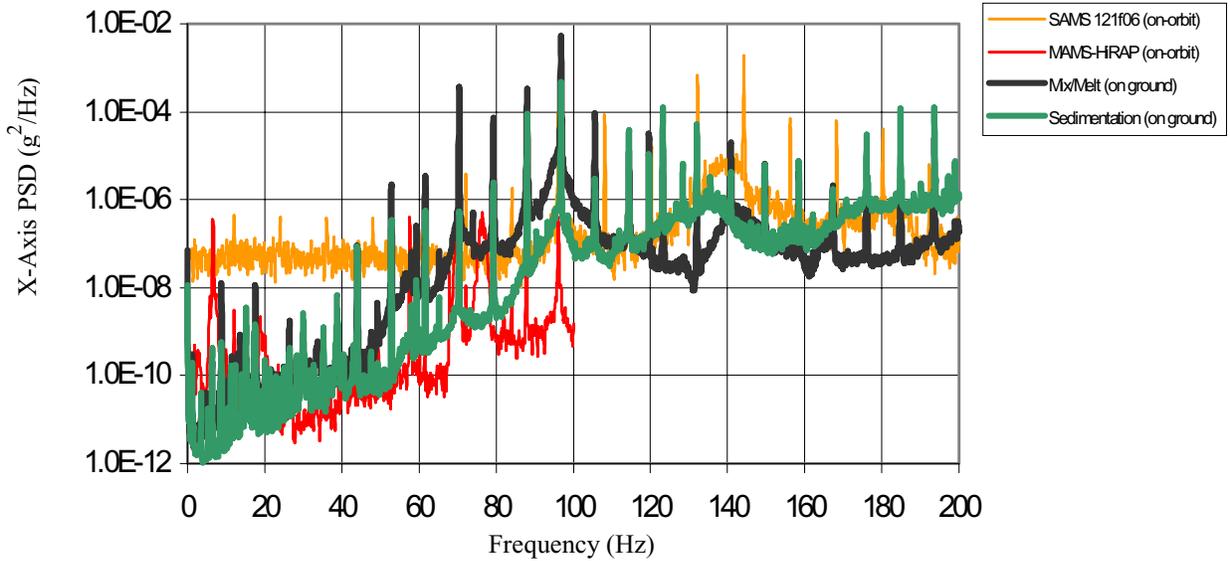| U.S. Lab: All Sources Operating, Except CDRA					
X-axis		Y-axis		Z-axis	
Frequency (Hz)	Acceleration (µg)	Frequency (Hz)	Acceleration (µg)	Frequency (Hz)	Acceleration (µg)
40.75	176.71	39.0	133.44	46.5	82.751
68.25	227.07	49.50	531.26	46.75	82.139
68.75	226.39	57.0	417.01	47.25	83.225
79.5	549.46	57.25	395.88	47.75	84.082
87.0	205.29	58.0	448.20	48.0	83.609
104.75	166.29	76.0	614.31	59.75	97.803
122.25	186.25	76.75	603.14	76.00	218.98
142.0	1728.4	94.50	269.7	76.75	212.87
153.25	156.78	98.00	1028.6	77.0	201.53
154.5	143.81	100.75	398.11	92.75	62.488
156.25	130.75	112.75	118.31	93.0	64.414
168.75	316.09	115.50	172.76	116.75	40.698
237.25	658.11	142.0	1035.60	117.0	42.055
254.50	594.24	166.50	690.38	117.75	44.657
256.75	599.42	168.75	747.36	132.0	93.234
269.75	656.03	170.0	851.49	132.25	98.548
284.0	6756.3	171.75	872.35	132.75	102.93
298.25	482.83	195.0	190.60	142.0	686.08
		204.25	242.00	170.0	112.15
		224.25	179.24	171.5	118.16
		224.50	177.73	179.25	52.031
		225.0	174.32	180.5	50.413
		242.5	147.79	218.50	158.14
		244.75	174.61	239.75	356.63
		245.50	192.11	240.75	349.58
		269.75	663.13	284.0	5111.2
		284.0	3552.9	298.25	362.46
		298.25	281.36		

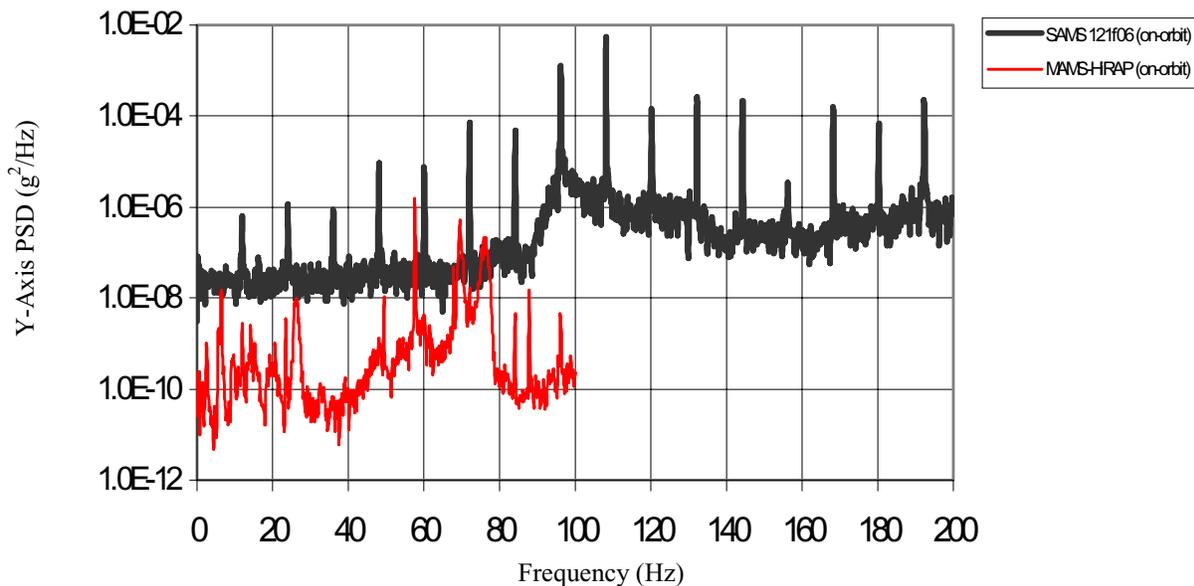Figure 4: PSD of EXPPCS On-orbit versus Ground Test Data For Two Different Sensors

Figure 5: PSD of EXPPCS On-orbit versus Ground Test Data For Two Different Sensors
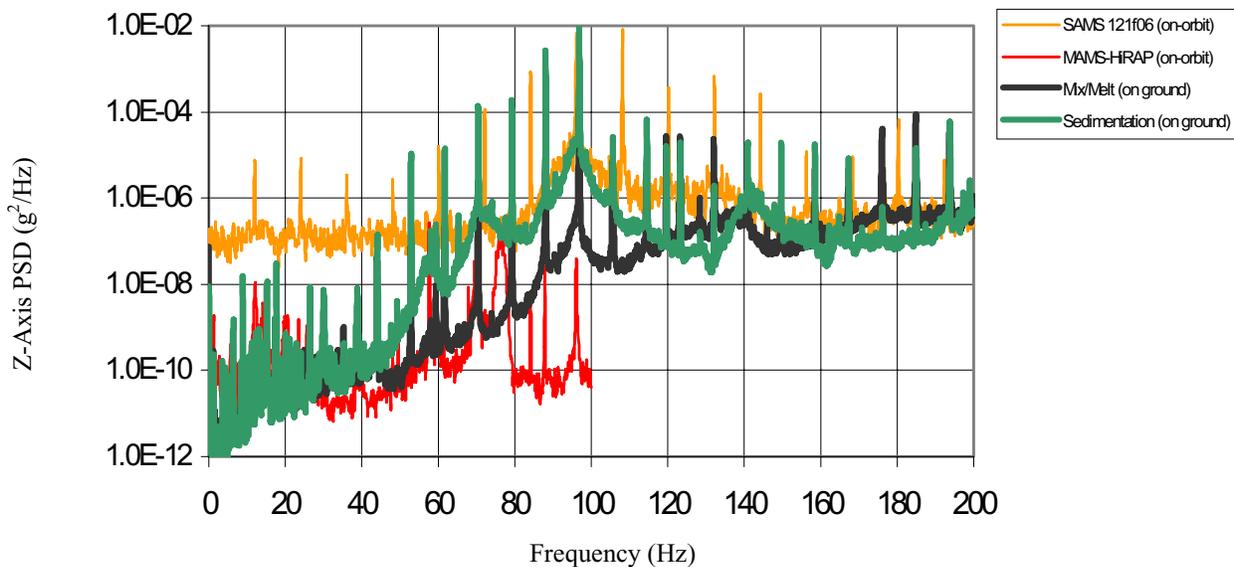

Figure 6: PSD of EXPPCS On-orbit versus Ground Test Data For Two Different Sensors

REPORT DOCUMENTATION PAGE

1. AGENCY USE ONLY (Leave blank)	2. REPORT DATE	3. REPORT TYPE AND DATES COVERED
	August 2002	Technical Memorandum

4. TITLE AND SUBTITLE

Monitoring the Microgravity Environment Quality On-Board the International Space Station Using Soft Computing Techniques

Part II: Preliminary System Performance Results

5. FUNDING NUMBERS

WU–400–35–4C–00

6. AUTHOR(S)

Kenol Jules, Paul P. Lin, and Daniel S. Weiss

7. PERFORMING ORGANIZATION NAME(S) AND ADDRESS(ES)

National Aeronautics and Space Administration
John H. Glenn Research Center at Lewis Field
Cleveland, Ohio 44135–3191

8. PERFORMING ORGANIZATION REPORT NUMBER

E–13509

9. SPONSORING/MONITORING AGENCY NAME(S) AND ADDRESS(ES)

National Aeronautics and Space Administration
Washington, DC 20546–0001

10. SPONSORING/MONITORING AGENCY REPORT NUMBER

NASA TM—2002-211813
IAF–01–J.5.01

11. SUPPLEMENTARY NOTES

Prepared for the 52nd International Astronautical Congress cosponsored by the International Astronautical Federation, French Academy of Sciences, Air & Space National Academy, Floral World Academy, and the Art & Literature Academy, Toulouse, France, October 1–5, 2001. Kenol Jules, NASA Glenn Research Center; Paul P. Lin, Cleveland State University, Cleveland, Ohio; and Daniel S. Weiss, Harvard University, Cambridge, Massachusetts. Responsible person, Kenol Jules, organization code 6727, 216–977–7016.

12a. DISTRIBUTION/AVAILABILITY STATEMENT

Unclassified - Unlimited
Subject Categories: 19 and 35   Distribution: Nonstandard

Available electronically at http://gltrs.grc.nasa.gov

This publication is available from the NASA Center for AeroSpace Information, 301–621–0390.

12b. DISTRIBUTION CODE

13. ABSTRACT (Maximum 200 words)

This paper presents the preliminary performance results of the artificial intelligence monitoring system in full operational mode using near real time acceleration data downlinked from the International Space Station. Preliminary microgravity environment characterization analysis result for the International Space Station (Increment-2), using the monitoring system is presented. Also, comparison between the system predicted performance based on ground test data for the US laboratory "Destiny" module and actual on-orbit performance, using measured acceleration data from the U.S. laboratory module of the International Space Station is presented. Finally, preliminary on-orbit disturbance magnitude levels are presented for the Experiment of Physics of Colloids in Space, which are compared with on ground test data. The ground test data for the Experiment of Physics of Colloids in Space were acquired from the Microgravity Emission Laboratory, located at the NASA Glenn Research Center, Cleveland, Ohio. The artificial intelligence was developed by the NASA Glenn Principal Investigator Microgravity Services Project to help the principal investigator teams identify the primary vibratory disturbance sources that are active, at any moment of time, on-board the International Space Station, which might impact the microgravity environment their experiments are exposed to. From the Principal Investigator Microgravity Services' web site, the principal investigator teams can monitor via a dynamic graphical display, implemented in Java, in near real time, which event(s) is/are on, such as crew activities, pumps, fans, centrifuges, compressor, crew exercise, structural modes, etc., and decide whether or not to run their experiments, whenever that is an option, based on the acceleration magnitude and frequency sensitivity associated with that experiment. This monitoring system detects primarily the vibratory disturbance sources. The system has built-in capability to detect both known and unknown vibratory disturbance sources. Several soft computing techniques such as Kohonen's Self-Organizing Feature Map, Learning Vector Quantization, Back-Propagation Neural Networks, and Fuzzy Logic were used to design the system.

14. SUBJECT TERMS

Learning vector quantization; Kohonen's self-organizing feature map

15. NUMBER OF PAGES

21

16. PRICE CODE

17. SECURITY CLASSIFICATION OF REPORT	18. SECURITY CLASSIFICATION OF THIS PAGE	19. SECURITY CLASSIFICATION OF ABSTRACT	20. LIMITATION OF ABSTRACT
Unclassified	Unclassified	Unclassified	